International Journal of Heat and Mass Transfer 52 (2009) 2667–2672

Contents lists available at ScienceDirect

International Journal of Heat and Mass Transfer

journal homepage: www.elsevier.com/locate/ijhmt

Experimental investigation of heat transfer in oscillating annular flow

Unal Akdag [a,*], A. Feridun Ozguc [b]

[a] Aksaray University, Mechanical Engineering Department, TR-68100 Aksaray, Turkey
[b] Istanbul Technical University, Faculty of Mechanical Engineering, Gumussuyu, TR-34437 Istanbul, Turkey

ARTICLE INFO

Article history:
Received 16 April 2008
Received in revised form 3 November 2008
Available online 21 February 2009

Keywords:
Oscillating flow
Annular channel
Heat transfer enhancement

ABSTRACT

Heat transfer from a surface having constant heat flux subjected to oscillating flow in a vertical annular liquid column is investigated experimentally. The oscillation of water column in annuli is created using a piston cylinder mechanism. The experiments are carried out for four different oscillation frequencies, three amplitudes and three heat fluxes while the other parameters remain constant. The cycle-averaged values are considered in the calculation of heat transfer using the control volume approximation. Based on the experimental data, an empirical equation is obtained for the cycle averaged Nusselt number as a function of kinetic Reynolds number and dimensionless amplitude.

1. Introduction

Heat and mass transfer in oscillating flow has been a principal investigation area for past several decades. Oscillation-induced heat transport processes maintain an effective heat enhancement. They have many important applications in compact heat exchangers, cryocoolers, Stirling engines, internal combustion machines and other periodical thermal systems. A wide literature survey in oscillating flow heat transfer and fluid flow characteristics is reported by Zhao and Cheng [1]. They investigated two different groups as a pulsating flow and reciprocating (zero-mean oscillating) flow. Pulsating flows are always unidirectional and can be separated into steady and unsteady components, such as blood flow in arteries [2]. For reciprocating flows, the flow direction changes cyclically. Hence, these flows convect zero net mass flow. Reciprocating flows occur in many reciprocating-motion machines such as internal combustion engines, Stirling engines and pulse tube cryocoolers. This study focused on zero-mean oscillatory flow.

Oscillating flow and heat transfer have been investigated by two different categories; namely axial diffusion with pure conduction and convection heat transfer. In the first one, the investigators focused on heat conduction enhancement due to high frequency and low amplitude oscillations. One of the early studies of this kind is due to Chatwin [3], who showed enhancement of species diffusion under high frequency oscillations. Later this phenomenon was applied to enhance heat transfer. Kurzweg [4] confirmed this conjecture and developed a new method using tube bundle between two hot and cold reservoirs by means of sinusoidal oscillations. Very large effective axial heat conduction rates were found, as well as exceeding those possible with heat pipes by several orders of magnitude [5–9]. Second category investigations are focused on forced convection with low frequency, large amplitude oscillations in relatively short channels. Among these studies, Cooper et al. [10] investigated experimentally the convective heat transfer from a heated floor section of a rectangular duct to a low frequency, large tidal displacement oscillating flow. The higher heat transfer rates were found for smaller duct heights, higher oscillation frequencies and large tidal displacement. Li and Yang [11] investigated heat transfer in oscillating flows at low frequencies and large amplitudes by numerical simulations using the experimental results of Cooper et al. A number of studies on convection heat transfer in oscillating flows, including experimental [12–14], and numerical [15–17] investigations have been reported the oscillating flow is a strong function of the frequency and amplitude of oscillations. This fact is verified by analytical studies of some investigators that employed simplifications for obtaining in oscillating flow temperature distribution [18–20].

Although the oscillatory flow heat transfer problem has an important application to the design of enhanced heat transfer devices, the experimental and numerical studies are scarce to achieve the full potential of oscillatory flow. In particular, the design of heat exchanger has been based on steady flow correlations, which are not suitable for reciprocating flow. New correlations are required to achieve improved designs of heat exchangers; already several novel heat exchanger devices for electronic cooling applications utilize oscillating flow and heat transfer [21–23].

In the present paper, the heat transfer from a surface subject to oscillating flow in a vertical annular channel is investigated experimentally. The experiments have been performed for a wide range of kinetic Reynolds number. The heat transfer from heater to water is calculated by means of the experimental data using control

* Corresponding author. Tel.: +90 382 2150953; fax: +90 382 2150592.
E-mail address: uakdag@gmail.com (U. Akdag).

0017-9310/$ - see front matter © 2009 Elsevier Ltd. All rights reserved.
doi:10.1016/j.ijheatmasstransfer.2009.01.006

Nomenclature

A	cross-sectional area of liquid column (m^2)
A_o	dimensionless oscillation amplitude ($A_o = 2x_m/D$)
A_p	cross-sectional area of piston (m^2)
c	specific heat of fluid (kJ/kg-K)
D	hydraulic diameter of test duct (m) ($D = 2(r_2\text{-}r_1)$)
h	heat transfer coefficient (W/m^2-K)
H_1, H_2	cycle-averaged enthalpies Eq. (6) (J)
k	thermal conductivity (W/m-K)
L	total distance from probe1 to probe2 (m)
l_h	heater length (m)
l_o	distance from probes to heater (m)
Pr	Prandtl Number ($Pr = \nu/\alpha$)
Q_k	total heat loss to environment over a cycle (J)
Q_l	total heat transferred to water over a cycle (J)
q_e	total wall heat flux (W)
q''_1	heat flux from heater to control volume (W/m^2)
q''_2	heat flux from glass tube to environment (W/m^2)
R	flywheel radius (m)
Re_ω	kinetic Reynolds number ($Re = \omega D^2/\nu$)
r	radial coordinate
r_1	inner radius of annulus (m)
r_2	outer radius of annulus (m)
x_m	oscillation amplitude (m)
t	time (s)
T	temperature
T_a	ambient temperature (°C)
T_b	bulk temperature (°C)
T_{ca}	temperatures of the outer surface of glass tube corresponding to air region of the test section (°C)
T_{cl}	temperatures of the outer surface of glass tube corresponding to water region of the test section (°C)
T_1	first probe temperatures (°C)
T_2	second probe temperatures (°C)
T_w	space-cycle averaged wall temperatures (°C)
T_m	averaged bulk temperature defined in Eq. (14) (°C)
u	mean velocity (m/s)
u_m	maximum velocity (m/s)
y	vertical coordinate
y^*	distance from reference to the meniscus (m)
z	Interface position (m)
z_o	oscillation axis or filling height (m)

Greek Symbols

α	thermal diffusivity of fluid (m^2/s)
δ	momentum boundary layer thickness (m)
ϕ	loss parameter defined in Eq. (8)
ρ	fluid density (kg/m^3)
ω	angular frequency (rad/s)
ν	kinematic viscosity (m^2/s)

Subscripts

l	liquid
a	air

volume approach. Then, an empirical equation of the cycle-averaged Nusselt number is obtained as function of kinetic Reynolds number and dimensionless amplitude. In the present study, the effects of new parameters on the heat transfer are investigated, different than previous studies [24,25]. The experimental results presented and the effects of various heat transfer parameters on oscillatory forced convection are discussed.

2. Experimental study

Fig. 1 shows a schematic diagram illustrating the experimental setup. The oscillatory flow system and the set-up were described in detail in a previous paper [24]. The annular test section preferred in order to ensure to the transfer all of given heat flux from heater to control volume. In setup, the outer part of the vertical annular test section is a glass tube of 2 m in length, 42 mm in outer diameter and 37.4 mm in inner diameter. A cylinder (18 mm in outer diameter) consisting of four zones such as heater, cooler and adiabatic parts, is located at the centerline of the glass tube. The cooler is made of copper tubes with lengths of 760 mm. One of the adiabatic parts is placed between heater and cooler. These zones are assembled together using threaded joints in order to obtain a smooth continuous surface.

The heater is built by embedding an electrical resistance inside the copper tube. The cables of six thermocouples located at the inner surface of the heater tube are taken out of the test section by passing them inside of the heater tube and the adiabatic Teflon tube above the heater. Thus, the flow disturbances which might have resulted from caused power and thermocouple cables are eliminated. Since thermocouple cables are located parallel to the electrical cables DC power is used to feed the heater in order to prevent thermocouples from electrical inductance.

The cooler is made of two concentric copper tubes. The cooling water enters the inner tube which is 8 mm in diameter and leaves from the outer tube of the cooler. Eight thermocouples are welded on the cooler surface and the leads are taken out of the test section by passing them through the cooling water [25].

The first temperature probe is located at the half of the adiabatic section between heater and cooler in order to measure the water temperature and to determine the enthalpy of the flow. This location is also the reference point to measure the positions of the surface temperatures and the interface (Fig. 2). This first probe consisting of four thermocouples located different positions across the annular gap. The second probe is the same as first one and it is positioned at 150 mm above the heater section. Each thermocouple signal of the probes is recorded and then the probe temperatures are calculated by averaging the thermocouple signals over the cross sectional area.

The outer surface temperatures of the glass tube are also measured by five thermocouples. All thermocouples are calibrated using a constant temperature bath to ensure the surface temperatures. A computer controlled data acquisition system (Keithley 2700) is used to collect data. The reciprocating motion of the water column is created using a piston–cylinder driven by a 1 kW DC motor with adjustable speed. The number of revolutions of the motor is measured by an optical digital tachometer. (Lutron DT-2234B). The filling height of the water column is kept constant for all cases, (z_o = 625 mm) [26].

3. Results and discussion

3.1. Liquid column velocity

It is observed that the motor frequency measured by tachometer is the same as the frequency of the recorded motion of the interface. While the maximum uniform velocity of the water column is $R\omega A_p/A = u_m$ as function of piston cross-sectional area, water column cross-sectional area, flywheel radius and frequency, the variation of the mean velocity of the liquid column with time can be written as follows:

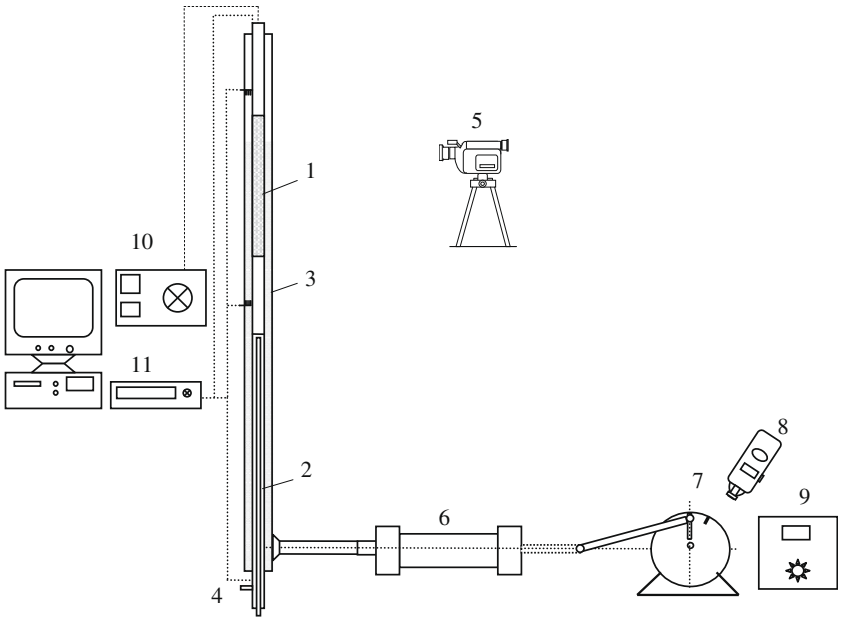

Fig. 1. Experimental setup: 1. heater, 2. cooler, 3. glass pipe, 4. cooling water inlet and outlet, 5. camera, 6. piston–cylinder apparatus, 7. DC motor, 8. dijital tachometer, 9. velocity control, 10. power supply, 11. data acquisition system (Keithley-2700).

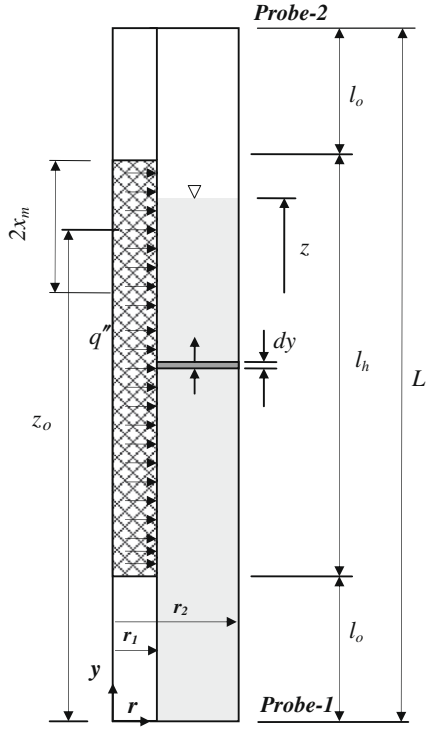

Fig. 2. Control volume and dimensions for experimental calculations.

$$u(t) = u_m \sin\omega t \tag{1}$$

It can be assumed that the interface is a flat surface by neglecting the capillary and wall effects. Then, the height z which shows the approximate position of the interface is derived easily by integration of Eq. (1) as:

$$z(t) = z_0 - x_m \cos\omega t \tag{2}$$

Here, $x_m = RA_p/A$ amplitude of z and z_o is the oscillation axis as shown in Fig. 2.

3.2. Calculation of the cycle-averaged heat transfer

In order to calculate the heat transfer from heater to fluid over a cycle, thermal energy balance is considered along the control volume, which is chosen the volume between the probe 1 and probe 2 as seen in Fig. 2.

A phase lag between boundary layer and core flow occurs of the nature of the reciprocating flow in the annular channel. The momentum boundary layer cannot follow the core simultaneously. The region that the inertial and viscous forces in the flow domain are equal is in the order of $\sqrt{2\nu/\omega}$. The momentum diffusion decreases quickly away from the wall. The penetration depth that senses the wall effects is approximately given by Zhao and Cheng [1] as follows:

$$\delta \cong 3\sqrt{2\nu/\omega} \tag{3}$$

This depth is below 1 mm for the frequencies considered in this study. Thus, the velocity profile can be assumed uniform in the annular channel. The thermal energy equation in the case of neglected the viscous dissipation and heat conduction in the flow direction (y-direction) can be written as follows:

$$\frac{\partial T}{\partial t} + u\frac{\partial T}{\partial y} = \alpha\frac{1}{r}\frac{\partial}{\partial r}\left(r\frac{\partial T}{\partial r}\right) \tag{4}$$

The differential equations are expressed in integral manner over the control volume. The integration of Eq. (4) over the cross sectional area, the following equation is obtained easily.

$$\frac{\partial T_b}{\partial t} + u\frac{\partial T_b}{\partial y} = \frac{2}{\rho c(r_2^2 - r_1^2)}(r_1 q_1'' - r_2 q_2'') \tag{5}$$

where q_1'', q_2'' are the heat fluxes on the heater surface and the outer surface of the glass tube, respectively. And the bulk temperature is defined by $T_b = \frac{1}{A}\int_A T(r,t)dA$.

The problem analyzing in this study is a conjugate heat transfer problem of the water–air system. The height z can indicate the position of the water–air interface approximately. In reality the water–air interface is not a flat surface because of the capillary and the water film created by the motion. Thus, the wetted heater surface can not be identified only by the z-position. Considering

the thermal energy conservation given by Eq. (4) for water and air regions can not give practical result individually, since the velocity at the each point of the surface on the interface are unknown. Thus, we consider the thermal energy equation for the whole system consisting of water and air regions together. If the Eq. (5) is integrated over the control volume shown in Fig. 2 and integrated over a cycle, we get:

$$H_2 - H_1 = \oint uA\rho_a c_a T_{ba}(L,t)dt - \oint uA\rho_l c_l T_{bl}(0,t)dt = q_1'' 2\pi r_1 l_h \left(\frac{2\pi}{\omega}\right) - \oint \int_0^L 2\pi r_2 q_2'' dy dt \quad (6)$$

Eq. (6) shows that the enthalpy difference over the control volume is equal to the heat transfer at the control volume surface. The heat flux from the heater to control volume is constant. But the heat flux from the glass wall to the environment is not constant; it varies with position and time. The last term on the right hand side of Eq. (6) shows the heat loss from the glass tube surface to the environment. The total heat loss over a cycle can be calculated by means of Eq. (6) as follows:

$$Q_k = \oint \int_0^L 2\pi r_2 q_2'' dy dt = q_1'' 2\pi r_1 l_h \left(\frac{2\pi}{\omega}\right) - (H_2 - H_1) \quad (7)$$

In this equation, the terms except heat loss term are calculated from experimental data.

It is clear that the surface temperatures of the inner side of the glass tube should vary harmonically with time. The variation of the measured surface temperatures of the outer side of the glass tube with time can be neglected as observed in the experiments. Although, outer surface temperatures have a negligible harmonic oscillation, it can be attributed to the damping effect of the glass wall.

The averaged surface temperature of the outer side of glass tube can be calculated from the measured values and it can be separated into two regions corresponding to the water and air regions with respect to the oscillation axis z_o. Thus, by using these averaged outer surface temperatures, the heat loss can be determined and separated into two parts approximately as follows by considering the Newton's cooling law.

$$\frac{Q_{kl}}{Q_k} = \frac{z_0(T_{cl} - T_a)}{z_0(T_{cl} - T_a) + (L - z_0)(T_{ca} - T_a)} = \phi \quad (8)$$

$$\frac{Q_{ka}}{Q_k} = \frac{(L - z_0)(T_{ca} - T_a)}{z_0(T_{cl} - T_a) + (L - z_0)(T_{ca} - T_a)} = (1 - \phi) \quad (9)$$

The thermal energy conservation equation for water region over a cycle without flat interface simplification can be written as follows:

$$H_1 = \oint \int_0^z 2\pi r_2 q_2'' dy\, dt - \oint \int_{l_0}^{y^*} 2\pi r_1 q_1'' dy\, dt \quad (10)$$

Here, y^* is the distance from reference to the meniscus. The first term on the right side of this equation shows the heat loss from the water side of the glass tube to the environment, so that Eq. (10) can be rearranged as:

$$Q_l = \oint \int_{l_0}^{y^*} 2\pi r_1 q_1'' dy\, dt = Q_{kl} - H_1 \quad (11)$$

Substituting Eqs. (7) and (8) in Eq. (11), the heat transfer to the water from the heater over a cycle is determined as:

$$Q_l = m_l q_1'' 2\pi r_1 l_h \left(\frac{2\pi}{\omega}\right) - \phi H_2 - (1 - \phi) H_1 \quad (12)$$

Cycle-averaged experimental data are given in the Table 1 with respect to the frequencies, amplitude and the heater power.

3.3. Prediction of Nusselt number

The total heat transfer to the water over a cycle Q_l, can be written as follows:

$$Q_l = 2\pi r_1 l_h h(T_w - T_m)(2\pi/\omega) \quad (13)$$

Here, the averaged water temperature can be defined as:

$$T_m = \frac{T_1 + T_2}{2} \quad (14)$$

T_1 and T_2 represent time-averaged probe temperatures as given in Table 1. Considering Eq. (13), the Nusselt number is defined as:

$$N_u = \frac{h l_h}{k} = \frac{l_h}{k} \frac{Q_l}{2\pi r_1 l_h (T_w - T_m)(2\pi/\omega)} \quad (15)$$

The calculated Nusselt numbers using Eq. (15) are given in Table 1 depend on experimental parameters.

Experimental results are shown the cycle averaged Nusselt number increases, while the increasing oscillation amplitude as shown in Fig. 3. At a higher value of A_o (A_o = 12.88) the maximum cross-sectional mean velocity is also high and forced convection effect predominate. However, at a lower value of A_o (A_o = 7.73) fluid velocity is low and forced convection effects become less significant respect to high values of A_o. Because, the temperature near the wall responds faster with respect to the velocity variation.

Nusselt number can be written as a function of kinetic Reynolds number ($Re_\omega = \omega D^2/\nu$), dimensionless oscillation amplitude ($A_o = 2x_m/D$), the length to diameter ratio of the heater (l_h/D) and Prandtl number [12].

$$Nu = f(Re_\omega,\ A_o,\ l_h/D,\ Pr)$$

In this study, the main parameters of oscillating flow, kinetic Reynolds number and dimensionless amplitude are considered as variables. The Prandtl number and geometric parameters kept constant for all cases. But, it is noted that in the literature decreasing the hydraulic diameter of pipe, the heat transfer is increased [7,9]. Based on the experimental data, the following correlation equation of the cycle averaged Nusselt number is obtained as:

$$Nu = 1.32 \mathrm{Re}_\omega^{0.248} A_o^{0.85} \quad (16)$$

and this equation is valid in the following range of kinetic Reynolds number and dimensionless amplitude.

$$1000 < Re_\omega < 4000 \text{ and } 7.73 < A_o < 12.88$$

The graphical representation of Eq. (17) is shown in Fig. 4. It is observed that, the cycle averaged Nusselt number increases with the increase of either the kinetic Reynolds number (Re_ω) or the dimensionless oscillation amplitude of fluid (A_o). The icrease in heat transfer is more sensitive to A_o than to Re_ω, since the exponent of A_o is greater than that of Re_ω.

3.4. Uncertainty analysis

An uncertainty analysis based on the method described by Holman [27] is performed. The uncertainty in the experimental data can be considered by identifying the main sources of errors in the measurements. The main source of errors in the reported results on the Nusselt number are statistical uncertainty power input, heater surface mean-temperatures and bulk temperature of fluid. The uncertainty in the Nusslet number is estimated as:

$$w_{Nu} = \left[\left(\frac{\partial Nu}{\partial Q_l} w_{Q_l}\right)^2 + \left(\frac{\partial Nu}{\partial T_w} w_{T_w}\right)^2 + \left(\frac{\partial Nu}{\partial T_m} w_{T_m}\right)^2 \right]^{1/2} \quad (17)$$

$$\frac{w_{Nu}}{Nu} = \left[\left(\frac{w_{Q_l}}{Q_l}\right)^2 + \left(\frac{w_{T_w}}{T_w}\right)^2 + \left(\frac{w_{T_m}}{T_m}\right)^2 \right]^{1/2} \quad (18)$$

Table 1
Cycle-averaged experimental data.

	ω (rad/s)	Re_ω	A_o	Q_e (W)	T_w (C)	T_1 (C)	T_2 (C)	ϕ	$-H_1$ (J)	H_2 (J)	Q_k (J)	Q_l (J)	h (W/m^2-K)	Nu	Uncertainty (%)
Exp-1	1.445	1026.11	12.88	50	50.19	27.64	36.20	0.77	126.91	0.14	90.37	196.19	66.39	60.54	10.69
Exp-2	2.712	1925.97	12.88	50	42.57	24.95	29.86	0.75	71.42	0.08	44.34	104.49	79.95	72.90	12.44
Exp-3	3.906	2773.70	12.88	50	39.13	24.16	27.03	0.75	50.65	0.06	29.72	73.02	90.13	82.18	13.02
Exp-4	5.130	3642.88	12.88	50	38.19	25.33	25.07	0.80	47.87	0.03	13.34	58.57	98.94	90.22	13.61
Exp-5	1.435	1018.73	12.88	100	75.13	34.79	48.03	0.76	182.22	0.17	255.59	377.68	68.74	62.68	5.67
Exp-6	2.723	1933.43	12.88	100	68.04	32.24	43.16	0.77	157.77	0.15	72.86	214.07	82.20	74.95	5.83
Exp-7	3.948	2803.46	12.88	100	60.25	30.61	35.85	0.79	82.38	0.05	76.72	143.34	89.61	81.71	6.71
Exp-8	5.130	3642.88	12.88	100	56.28	30.46	32.84	0.79	57.98	0.03	64.47	109.00	97.13	88.57	7.24
Exp-9	1.434	1018.30	12.88	150	102.02	41.44	59.37	0.78	348.76	0.47	308.01	590.00	70.13	63.95	3.76
Exp-10	2.723	1933.43	12.88	150	86.90	37.49	47.34	0.79	201.11	0.21	144.83	315.46	82.61	75.33	4.00
Exp-11	3.958	2810.63	12.88	150	78.67	36.09	40.06	0.80	150.14	0.07	87.91	220.05	91.78	83.69	4.37
Exp-12	5.130	3642.88	12.88	150	75.19	34.80	35.37	0.82	132.42	0.01	51.29	174.35	95.42	87.01	4.42
Exp-13	1.435	1018.73	10.30	50	70.86	29.86	36.05	0.82	109.79	0.14	109.06	199.21	32.26	29.42	7.27
Exp-14	2.723	1933.43	10.30	50	49.10	27.21	34.49	0.81	72.27	0.08	43.04	107.27	68.46	62.43	10.45
Exp-15	3.958	2810.63	10.30	50	45.35	25.69	31.54	0.81	54.71	0.06	24.61	74.52	75.42	68.77	11.19
Exp-16	5.099	3620.87	10.30	50	42.74	25.12	28.55	0.81	44.43	0.03	17.15	58.32	79.99	72.94	11.67
Exp-17	1.424	1011.20	10.30	100	90.00	35.85	57.63	0.80	219.92	0.17	221.14	397.45	55.98	51.04	4.95
Exp-18	2.712	1925.83	10.30	100	76.00	32.59	49.09	0.81	128.51	0.15	103.02	211.51	69.79	63.64	5.50
Exp-19	3.958	2810.63	10.30	100	70.24	30.27	44.10	0.81	95.83	0.05	62.86	146.63	75.12	68.49	5.65
Exp-20	5.130	3642.88	10.30	100	66.56	31.20	37.61	0.82	81.57	0.03	40.87	115.08	78.56	71.63	5.79
Exp-21	1.445	1026.11	10.30	150	122.05	44.05	74.58	0.82	312.03	0.47	339.73	589.58	58.10	52.98	3.19
Exp-22	2.723	1933.43	10.30	150	102.30	40.08	62.72	0.82	173.80	0.21	172.14	314.28	71.93	65.59	3.58
Exp-23	3.958	2810.63	10.30	150	94.50	40.44	51.65	0.83	140.11	0.07	97.94	221.11	77.27	70.46	3.60
Exp-24	5.131	3643.80	10.30	150	87.00	39.11	45.41	0.84	106.00	0.01	77.66	171.17	83.99	76.59	3.86
Exp-25	1.435	1018.73	7.73	50	67.39	31.27	45.81	0.88	110.73	0.14	108.12	205.65	43.74	39.89	7.92
Exp-26	2.723	1933.43	7.73	50	58.10	29.57	38.24	0.88	67.39	0.08	47.92	109.71	52.82	48.16	8.38
Exp-27	3.958	2810.63	7.73	50	55.03	29.76	37.69	0.88	52.78	0.06	26.54	76.25	60.61	55.27	8.81
Exp-28	5.142	3651.19	7.73	50	51.78	28.92	34.83	0.89	42.76	0.03	18.31	58.99	65.19	59.44	9.21
Exp-29	1.435	1018.73	7.73	100	109.00	41.01	68.51	0.86	175.76	0.17	262.04	400.69	45.34	41.34	4.12
Exp-30	2.723	1933.43	7.73	100	92.77	37.97	54.89	0.86	106.14	0.15	124.49	213.75	53.72	48.99	4.44
Exp-31	3.875	2751.40	7.73	100	84.18	35.01	51.75	0.86	82.07	0.05	80.05	151.03	61.36	55.95	4.54
Exp-32	5.130	3642.88	7.73	100	80.57	35.13	46.85	0.87	69.19	0.03	53.25	115.64	64.12	58.46	4.63
Exp-33	1.435	1018.73	7.73	150	141.59	43.84	83.50	0.86	341.62	0.47	314.88	611.07	48.14	43.89	2.71
Exp-34	2.712	1925.97	7.73	150	129.67	42.59	81.77	0.85	192.57	0.21	154.72	324.85	55.85	50.93	2.85
Exp-35	3.958	2810.63	7.73	150	118.10	41.18	70.76	0.86	141.50	0.07	96.55	225.01	61.32	55.92	3.01
Exp-36	5.130	3642.88	7.73	150	111.26	41.16	63.52	0.86	119.57	0.01	64.14	174.92	65.15	59.41	3.12

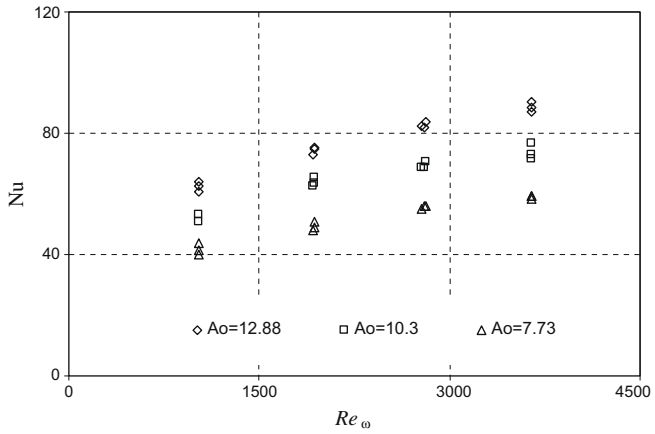

Fig. 3. Effects of the dimensionless oscillation amplitude on the cycle averaged Nusselt number.

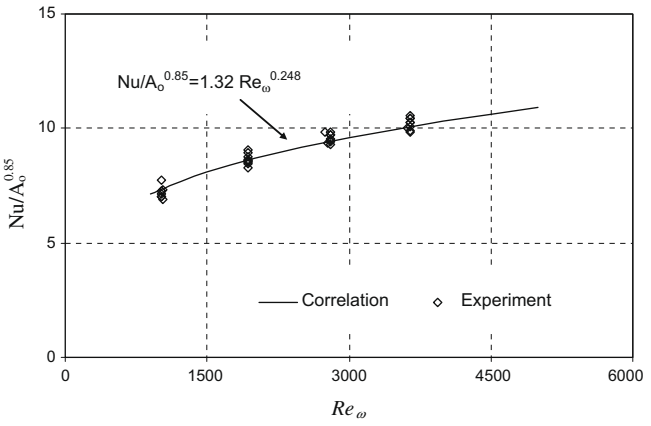

Fig. 4. An empirical equation based on the experimental data for the cycle averaged Nusselt number in oscillating annular flow.

The estimated uncertainties in the power output, heater surface mean-temperature and bulk-temperature of fluids are 6.2, 1.34 and 0.35%, respectively. The oscillation frequency of the water column is equal to motor drive, and so it is neglected. Finally, the calculated uncertainties for Nusslet number are given in Table 1 a different column with all experimental data.

4. Conclusion

In this study, the heat transfer from a heated surface in an oscillating vertical annular liquid column is investigated experimentally. The experiments are carried out for different frequencies, amplitude (A_o) and heat fluxes (q_e) while the Prandtl number (Pr) and geometric parameter ($l_h/D = 30$) remain constant. All the mathematical calculations in analyzing the experimental data are based on measurements taken from the test section considered as the control volume shown in Fig. 2. A correlation for cycle-averaged Nusselt number has been obtained from the experimental data. The heat transfer increases with increasing both the frequency and amplitude of the oscillation. It can be concluded that the oscillating flow heat transfer depends significantly on the frequency and amplitude. The present results will contribute for the design of heat exchanger like Stirling engines, pulse-tube refrigerator

and control of heat transfer equipment. It is interesting to note that, this heat transfer method will be applicable to heat transfer control mechanism by regulating the frequency and amplitude.

References

[1] T.S. Zhao, P. Cheng, Heat transfer in oscillatory flow, Ann. Rev. Heat Transfer IX (1998) (Chapter 7).
[2] M. Zamir, The Physics of Pulsatile Flow, Springer-Verlag, New York, 2000.
[3] P.C. Chatwin, On the longitudinal dispersion of passive contaminant in oscillatory flows in tubes, J. Fluid Mech. 71 (3) (1975) 513–527.
[4] U.H. Kurzweg, Enhanced heat conduction in fluids subjected to sinusoidal oscillations, J. Fluid Mech. 156 (1985) 291–300.
[5] U.H. Kurzweg, Temporal and spatial distribution of heat flux in oscillating flow subjected an axial temperature gradient, ASME, J. Heat Transfer 29 (1986) 969–1977.
[6] U.H. Kurzweg, L.D. Zhao, Heat transfer by high-frequency oscillations: a new hydrodynamic technique for achieving large effective thermal conductivities, Phys. Fluids 27 (11) (1984) 2624–2627.
[7] J.G. Zhang, U.H. Kurzweg, Numerical simulation of time-dependent heat transfer in oscillating pipe flow, J. Thermophys. 5 (1990) 401–406.
[8] M. Ozawa, A. Kawamoto, Lumped-parameter modeling of heat transfer enhanced by sinusoidal motion of fluid, Int. J. Heat Mass Transfer 34 (12) (1991) 3083–3095.
[9] S. Nishio, X.H. Shi, W.M. Zhang, Oscillation-induced heat transport: heat transport characteristics along liquid-columns of oscillation-controlled heat transport tubes, Int. J. Heat Mass Transfer 38 (13) (1995) 2457–2470.
[10] W.L. Cooper, V.W. Nee, K.T. Yang, An experimental investigation of convective heat transfer from the heated floor of a rectangular duct to a low frequency, large tidal displacement oscillatory flow, Int. J. Heat Mass Transfer 37 (4) (1994) 581–592.
[11] P. Li, K.T. Yang, Mechanisms for the heat transfer enhancement in zero-mean oscillatory flows in short channels, Int. J. Heat Mass Transfer 43 (19) (2000) 3551–3566.
[12] T.S. Zhao, P. Cheng, Ocillatory heat transfer in a pipe subjected to a laminar reciprocating flow, ASME J. Heat Transfer 118 (1996) 509–511.
[13] S.G. Qiu, T.W. Simon, Measurements of heat transfer and fluid mechanics within an oscillatory flow in a pipe, in: Fundamentals of Heat Transfer in Forced Convection, HTD 285, ASME, New York, 1994, pp. 1–7.
[14] T.E. Walsh, K.T. Yang, V.W. Nee, Q.D. Liao, Forced convection cooling in microelectronic cabinets via oscillatory flow techniques, in: Exp. of Heat Transfer, Fluid Mech. and Thermo, Elsevier, Amsterdam, 1993, pp. 641–648.
[15] T.S. Zhao, P. Cheng, A numerical solution of laminar forced convection in a heated pipe subjected to a reciprocating flow, Int. J. Heat Mass Transfer 38 (16) (1995) 3011–3022.
[16] C. Sert, A. Beskok, Numerical simulation of reciprocating flow forced convection in two-dimensional channels, ASME, J. Heat Transfer 125 (2003) 403–412.
[17] J.G. Zhang, U.H. Kurzweg, Numerical simulation of time-dependent heat transfer in oscillatory pipe flow, AIAA J. Thermophys. Heat Transfer 5 (1991) 401–406.
[18] D. Gedeon, Mean-parameter modelling of oscillating flow, ASME J. Heat Transfer 107 (1986) 513–518.
[19] R. Siegel, Influence of oscillation-induced diffusion on heat transfer in a uniformly heated channel, ASME J. Heat Transfer 109 (1987) 244–246.
[20] D.Y. Lee, S.J. Park, S.T. Ro, Heat transfer in the thermally developing region of a laminar oscillating pipe flow, Cryogenics 38 (1998) 585–594.
[21] T.W. Simon, J.R. Seume, A survey of oscillating flow in Stirling engine heat exchangers, NASA Contractor Report 182108, 1988.
[22] M. Kavinay, Performance of a heat exchanger based on enhanced heat diffusion in fluids by oscillation: analysis, ASME J. Heat Transfer 112 (1990) 49–55.
[23] M. Kavinay, M. Reckker, Performance of a heat exchanger based on enhanced heat diffusion in fluids by oscillation: experiment, ASME J. Heat Transfer 112 (1990) 56–63.
[24] U. Akdag, M. Ozdemir, Heat transfer in an oscillating vertical annular liquid column open to atmosphere, Heat Mass Transfer 42 (7) (2006) 617–624.
[25] U. Akdag, M. Ozdemir, A.F. Özgüc, Heat removal from oscillating flow in a vertical annular channel, Heat Mass Transfer 44 (4) (2008) 393–400.
[26] U. Akdag, Investigation of heat transfer in moving liquid column, PhD Thesis, Istanbul Technical University, Istanbul, Turkey, 2005. (in Turkish).
[27] J.P. Holman, Experimental Methods for Engineers, McGraw-Hill, New York, 2001.